SUPPORTING INFORMATION

Exposure assessment for estimation of the global burden of disease attributable to outdoor air pollution

Michael Brauer[1*], Markus Amann[2], Rick T. Burnett[3], Aaron Cohen[4], Frank Dentener[5], Majid Ezzati[6], Sarah B. Henderson[7], Michal Krzyzanowski[8], Randall V. Martin[9,10], Rita Van Dingenen[5], Aaron van Donkelaar[9], George D. Thurston[11] on behalf of the Outdoor Air Pollution Expert Working Group of the Global Burden of Disease Project

[1]School of Population and Public Health, The University of British Columbia, 2206 East Mall, Vancouver, BC, V6T1Z3 Canada
[2] International Institute for Applied Systems Analysis (IIASA), Schlossplatz 1 A-2361,Laxenburg, Austria
[3] Biostatistics and Epidemiology Division, Health Canada, 203 Environmental Health Center, Tunney's Pasture, Ottawa, ON, Canada K1A 0L2.
[4] Health Effects Institute, Boston USA
[5]European Commission, Joint Research Centre, Institute for Environment and Sustainability, 21027 Ispra, Italy
[6]Imperial College London, School of Public Health, Norfolk Place,
London W2 1PG UK
[7]British Columbia Centre for Disease Control, 655 West 12th Avenue
Vancouver, BC V5Z4R4 Canada
[8]World Health Organization, European Centre for Environment and Health, Hermann-Ehlers-Str. 10 53113 Bonn, Germany
[9]Dalhousie University, Department of Physics and Atmospheric Science, 6310 Coburg Road, Halifax, NS, B3H 3J5 Canada
[10] Harvard-Smithsonian Center for Astrophysics, 60 Garden Street, Cambridge, MA 02138 , USA
[11]New York University, Institute of Environmental Medicine, 57 Old Forge Road, Tuxedo, NY 10987 USA

*Corresponding Author
Michael Brauer
School of Population and Public Health
The University of British Columbia
3rd Floor- 2206 East Mall
Vancouver BC V6T1Z3 Canada
Tel 604 822 9585
michael.brauer@ubc.ca

Pages: 27
Tables: 3
Figures: 7

Database

A comma-separated file containing all of the individual grid-cell estimates is available for download. A data dictionary (data methods.pdf) is also included as a separate file.

TM5

TM5 is a complex 3-dimensional global atmospheric chemical transport model that simulates the transport, chemical (trans)formation and wet and dry deposition of atmospheric trace gases and chemically active species (e.g. ozone, SO_2, NO_x, VOCs), as well as PM. The version used in this study describes the physical and chemical processes that lead to the formation and destruction of ozone, as well as individual chemical components that constitute PM, including: SO_4^{2-}, NO_3^-, NH_4^+, primary $PM_{2.5}$ and its components black carbon, organic carbon, sea salt, and mineral dust. Following the AEROCOM recommendations (1) a simplified parameterization for secondary organic aerosol is considered. The TM5 model includes coupled gas-phase chemistry and bulk (i.e. not size-resolved) PM chemistry, with the exception of dust and sea salt which are size-resolved, assuming lognormal size distributions from which their $PM_{2.5}$ fraction were derived. Anthropogenic PM components are assumed to be entirely within the $PM_{2.5}$ size fraction. The model is used for global studies that require high regional resolution (1°x1°) with coarser global resolution (6°x4°) being acceptable (2). The zoom algorithm introduces refinement in both space and time in some predefined regions, in this case Europe, North America and Asia.

The TM5 model operates with off-line meteorology from the European Centre for Medium range Weather Forecasts (ECMWF; 6 hours IFS forecast). These data are stored at a 6-hourly resolution for large scale 3D fields, and 3-hourly for parameters describing exchange processes at the surface. Of the 60 vertical layers in the ECMWF model, a subset of 25 layers is used within TM5, including 5 boundary layers, 10 free tropospheric layers, and 10 stratospheric layers. All TM5 runs were performed with emissions for 1990 and 2005, while using meteorology for 2001 as a representative period. The time resolution of the output is matched according to the definition of the exposure metrics: for PM, monthly means were stored and averaged annually. O_3 was stored as hourly means for the calculation of exposure metrics based on daily maximum levels.

In addition to meteorological data, the key inputs to TM5 are global gridded emissions (at a spatial resolution of 1°x1°). Urban areas are considered to be 'high emission areas' for primary $PM_{2.5}$ emissions, leading to an increment in the $PM_{2.5}$ concentration compared with the rural background (the so-called 'urban increment'). If an urban area occupies only a fraction of a 1°x1° grid cell, an emission and concentration gradient between the urban area and its rural background will exist within the grid cell that is not resolved by the TM5 model.

In order to better evaluate the urban exposure to $PM_{2.5}$, a sub-grid parameterization is applied to redistribute the urban and rural $PM_{2.5}$ concentrations, while maintaining the average native grid cell concentration (see also (3)).
A parameterization of the urban increment for (non-reactive) primary emitted $PM_{2.5}$ anthropogenic was been implemented by scaling the sub-grid emission strength of those

compounds to urban and rural sub-grids within the native grid cell. The model aggregates 0.1° x 1° emissions into 1 ° x 1° resolution and then transports these emissions and products. The sub-grid parameterization is based on population utilizes the information that was lost in the aggregation step. This is accomplished using a high-resolution (0.042°x0.042°) population dataset (GPW3, Center for International Earth Science Information Network, Columbia University, http://sedac.ciesin.columbia.edu/gpw) to subdivide the 1°x1° native grid in 24x24 subgrids. In this process, population density is used as a proxy to identify high emission ("urban") areas within each 1°x1° grid cell. A subgrid is labeled as 'urban' if the population density exceeds 600/km², and 'rural' otherwise. Specifically, let f_{UP} be the urban population fraction, defined as the fraction of the population within the native grid cell which resides in the urban-flagged sub-grids, and f_{UA} the urban area fraction, being the fraction of the native grid area occupied by the urban-flagged sub-grids (the number of urban sub-grids divided by the total number of sub-grids). Let E_P be the emission strength of the anthropogenic primary $PM_{2.5}$ of the whole native grid cell. The assumption is made that the fraction $f_{UP}.E_P$ is emitted from area $f_{UA}.A$ (A being the grid cell area) and $(1- f_{UP}).E_{BC}$ from area $(1- f_{UA}).A$.

Under steady-state conditions, neglecting the incoming concentration of $PM_{2.5}$ from neighbouring grid cells, the native grid-average primary $PM_{2.5}$ concentration can be written as:

$C_{P,av} = \frac{E_P}{\lambda}$ with λ = ventilation factor.

Assuming the ventilation factor λ is also valid for the urban and rural part of the grid cell (equivalent with the assumption that mixing layer height and wind speed are the same), the steady-state concentration in the urban and rural sub-areas can be written as:

$$C_{P,URB} = \frac{f_{UP}}{f_{UA}} \frac{E_P}{\lambda} \text{ and } C_{P,RUR} = \frac{(1 - f_{UP})}{(1 - f_{UA})} \frac{E_P}{\lambda}$$

The ventilation factor λ, including an implicit correction factor for the non-zero background concentration in neighbouring cells, is obtained by taking advantage of the explicitly modelled grid cell concentration with the air quality model $C_{P,av}$:

$$\lambda = \frac{E_P}{C_{P,av}}$$

Hence,

$$C_{P,URB} = \frac{f_{UP}}{f_{UA}} C_{P,av} \text{ and } C_{P,RUR} = \frac{(1 - f_{UP})}{(1 - f_{UA})} C_{P,av}$$

In order to avoid artificial spikes in urban concentrations when occasionally a very small fraction of the native grid cell contains a very large fraction of the population, empirical bounds are applied on the adjustment factors:

1) rural primary $PM_{2.5}$ *($C_{P,RUR}$)* should not be lower than 0.5 times the native grid average;
2) urban primary $PM_{2.5}$ should not exceed the rural concentration by a factor 5.

In any case, the urban and rural adjustments for the primary $PM_{2.5}$ fulfill the condition:

$$f_{UA}C_{URB} + (1 - f_{UA})C_{RUR} = C_{av}$$

All secondary components (SO_4, NO_3) and primary natural PM (mineral dust, sea salt) are assumed to be distributed uniformly over the native grid cell and hence are not incremented

The TM5 1°x1° fields are then interpolated to 0.1°x0.1° resolution, and for the relevant grid cells, the urban and rural $PM_{2.5}$ are assigned to the respective corresponding sub-grid cells. TM5 runs were performed with emissions for 1990 and 2005 from IIASA-GAINS, while using meteorology for 2001. 2001 meteorology for TM5 was chosen to be consistent with HTAP, and since substantial analysis has already been performed on this year. In addition it seems that 2001 was a rather 'standard' year for these two decades in most regions of the world (4). An overview of global emissions of key components is given in Table S1:

Table S1. Global anthropogenic emissions derived from a preliminary version of the GEA/GAINS inventory for 2005, and the AR5 emissions for 1990 (5). The Global Energy Assessment (GEA) report will be released in 2012.

PM2.5 [Tg/yr] 1990	PM2.5 [Tg/yr] 2005	SO2 [Tg SO2/yr] 1990	SO2 [Tg SO2/yr] 2005	NOX [Tg NO2/yr] 1990	NOX [Tg NO2/yr] 2005	VOC [Tg/yr] 1990	VOC [Tg/yr] 2005
70.17	**69.68**	**128.06**	**107.67**	**122.57**	**111.40**	**212.08**	**195.12**

SAT

The satellite-based approach used here extends that of Liu et al. (6) and van Donkelaar et al. (7) by combining multiple satellite instruments, using higher resolution observations, assessing the error in the estimate and including a global evaluation. Satellite observations that exhibit a monthly mean AOD bias versus AERONET (8) above +/- 0.1 or 25% by region are removed. These regions are defined by spectral ratios of surface albedo observed by MODIS (9). The remaining MODIS and MISR measurements are then averaged to produce a daily AOD map to be related to $PM_{2.5}$. Ground-based measurements of $PM_{2.5}$ for 2001-2006 from multiple networks show significant coincident agreement with satellite-derived $PM_{2.5}$ over North America (slope = 1.07; r = 0.77) and non-coincident agreement with the rest of the world (slope = 0.86; r = 0.83). Globally, satellite-derived estimates outperform GEOS-Chem simulations (slope = 0.54; r = 0.63), reflecting improvement for both fine resolution and large-scale features (10). The 2005 estimates for the GBD were prepared as a 2004-2006 average and corrected for sampling bias by the ratio of coincident and continuously sampled GEOS-Chem simulated values. The additional years of 2004 and 2006 were included to increase the number of observations being used in the SAT estimate, and to reduce the effects of interannual variation.

The GEOS-Chem model (http://geos-chem.org) solves for the temporal and spatial evolution of aerosol and gaseous compounds using meteorological data sets, emission inventories, and equations that represent the physics and chemistry of the atmosphere. We use GEOS-Chem v8-01-04 with assimilated meteorology from the Goddard Earth Observing System (GEOS-4) at the NASA Global Modeling Assimilation Office (GMAO) with a timestep of 15 minutes at a resolution of 2° x 2.5° and 42 vertical levels ranging between the surface and approximately 80 km. The lowest layer thickness is approximately 100 meters.

The GEOS-Chem aerosol simulation includes the sulfate-nitrate-ammonium system (11), primary (12) and secondary (13) carbonaceous aerosols, mineral dust (14) and sea-salt(15). The model has been extensively evaluated with ground-based measurements, including sulphate-ammonium-nitrate (e.g. ((11, 16, 17)), primary organic carbon and black carbon (e.g. (12, 18)) and dust (e.g. (14)). Aircraft measurements have also been used for evaluation (e.g. (18-21)).

Global anthropogenic emissions for 2005 are based on the EDGAR3.2 emission inventory (22), overlaid by the NEI2005 (http://www.epa.gov/ttn/chief/net/2005inventory.html), CAC2005 (http://www.ec.gc.ca/pdb/cac/), BRAVO (23), EMEP (http://www.emep.int/) and Streets (24, 25) regional inventories. Emissions for 1990 are based on the GEIA (26) emission inventory, overlaid by EMEP over Europe. SOx, NOx and CO emissions of both global and regional inventories are adjusted from their respective base year to the year to simulation using adjustment factors derived from local government emission estimates (20). Where government estimates are unavailable, CO_2 emissions from solid (SOx), total (NOx) and liquid (CO) sources used to represent annual changes. Anthropogenic black and organic carbon emissions are based on Bond et al. (27).

Backscaling of the satellite-derived $PM_{2.5}$ estimates is based upon the ratio of $PM_{2.5}$ simulated from 2005 and 1990 anthropogenic emissions. Meteorology and natural emissions, such as dust and biomass burning, are maintained at 2004-6 conditions for both simulations to minimize the impact of meteorologically-driven changes.

PM Measurements

A set of PM observations was assembled in support of this study. The data consists of a worldwide set of georeferenced annual average $PM_{2.5}$ values representing urban background concentrations largely drawn from readily available official monitoring networks for 2005 (and where data for 2005 were unavailable, for 2004-2006). Literature sources and personal communications were also used, especially in locations without regional/national monitoring networks. For a number of locations, $PM_{2.5}$ was not measured directly but was estimated based on PM_{10} measurements using $PM_{2.5}$:PM_{10} ratios .Where available, local (or country-specific, to reflect differences that may relate to the regional contributions of coarse PM) $PM_{2.5}$:PM_{10} ratios were used for all locations within a particular country. Elsewhere, a ratio of 0.5 was used, which was the default in the previous global burden estimates (28) and which approximates mean ratios for regions with large numbers of coincident measurements. Given the uncertainties inherent in estimating $PM_{2.5}$ from PM_{10} by this simple ratio method, the estimated PM concentrations should be used cautiously, especially in areas with high levels of dust.

Table S2 presents the number of locations with observations by region. No observations were included for the Asia Central, Carribean, Latin American Andean, Oceania, Sub-Saharan Africa Central, and Sub-Saharan Africa East regions.

Table S2. Number of locations with PM observations included in global measurement database.

Region Name	Measured $PM_{2.5}$	Estimated from PM_{10}
Asia Pacific, High Income	2	5
Asia East	2	115
Asia South	3	18
Asia Southeast	9	7
Australasia	23	0
Europe Central	26	0
Europe Eastern	0	0
Europe Western	141	0
Latin America Central	3	16
Latin America Southern	0	5
Latin America Tropical	1	0
North Africa/Middle East	2	7
North America High Income	263	23
Sub-Saharan Africa Southern	0	7
Sub-Saharan Africa West	0	1

Data sources:
European Union: Airbase database: http://www.eea.europa.eu/data-and-maps/data/airbase-the-european-air-quality-database-3 (accessed June 30, 2011)

Australia: National Environmental Proptection Measures, Ambient Airt Quality Monitoring Reports (2005) (http://www.ephc.gov.au/taxonomy/term/34 (accessed June 30, 2011).

Brazil: Sao Paulo: http://www.cetesb.sp.gov.br/Ar/publicacoes.asp; Other locations obtained via personal communication from Nelson Gouveia, University of Sao Paulo.

Canada: National Air Pollution Surveillance (NAPS) Network Annual Data Summary for 2005-2006 (http://www.etc-cte.ec.gc.ca/publications/naps/naps2005_annual.pdf (accessed June 30, 2011).
Chile: Programa de Control de Monitoreo de Calidad de Aire Nacional, Etapa 2005 Anuario de Calidad de Aire 2005 Preparado para COMISION NACIONAL DEL MEDIO AMBIENTE

China: National Statistics Communique 2005. Obtained via personal communication from Hao Jiming, Tsinghua University

Colombia: DOCUMENTO SOPORTE NORMA DE CALIDAD DEL AIRE, SUBDIRECCIÓN DE ESTUDIOS AMBIENTALES, IDEAM, Bogotá, 13 de Noviembre de 2005.

Egypt: Egypt State of the Environment Report 2005, http://www.eeaa.gov.eg/english/reports/SOE2006En/1-air/01-air%20pollution/01-air%20pollution.pdf (accessed June 30, 2011)

Ghana: Progress Report for the African Air Quality Monitoring Program. USEPA/USAID/UNEP/Ghana EPA. RTI International. 2006.

Israel: Obtained via personal communication from Levana Kordova – Biezuner, Scientific Director Israeli Air Monitoring Network, Air Quality Division, Ministry of Environmental Protection, State of Israel.

Kuwait (29), Lebanon (30),

Mexico, Bogota: data from ESCALA project obtained via personal communication from Isabelle Romieu, National Institute of Public Health, Mexico.

New Zealand: Environment Canterbury, Annual ambient air quality monitoring report 2005 (http://ecan.govt.nz/publications/Reports/AnnualAirQualityrpt05.pdf (accessed June 30, 2011); Environment New Zealand 2007 (http://www.mfe.govt.nz/publications/ser/enz07-dec07/html/chapter7-air/page3.html (accessed June 30, 2011)

South Africa: Durban: ETHEKWINI AIR QUALITY MONITORING NETWORK ANNUAL REPORT 2005 (http://www2.nilu.no/AirQuality/data/reports/%7BAD57131B-BCDC-BAD1-AEF6-8ABC376A16B5%7D.pdf (accessed June 30, 2011); Johannesburg: STATE OF THE

AIR REPORT City of Johannesburg (http://www.joburg-archive.co.za/2007/pdfs/air_quality/stateofair2007.pdf(accessed June 30, 2011)

United States: Air Quality Statistics by City (http://www.epa.gov/air/airtrends/factbook.html (accessed June 30, 2011).

Other Asian locations: (31); Data compiled by Clean Air Initiative Asia (www.cai-asia.org).

GBD Regions

21 regions were defined based on the following principles and are listed in the GBD Operations Manual, including the specific countries included in each region. (http://www.globalburden.org/GBD_Study_Operations_Manual_Jan_20_2009.pdf)

1. All regions are based on broad geographic regions or continents.

2. All regions have at least two countries.

3. Countries are grouped based on child and adult mortality levels and major causes of death in each country.

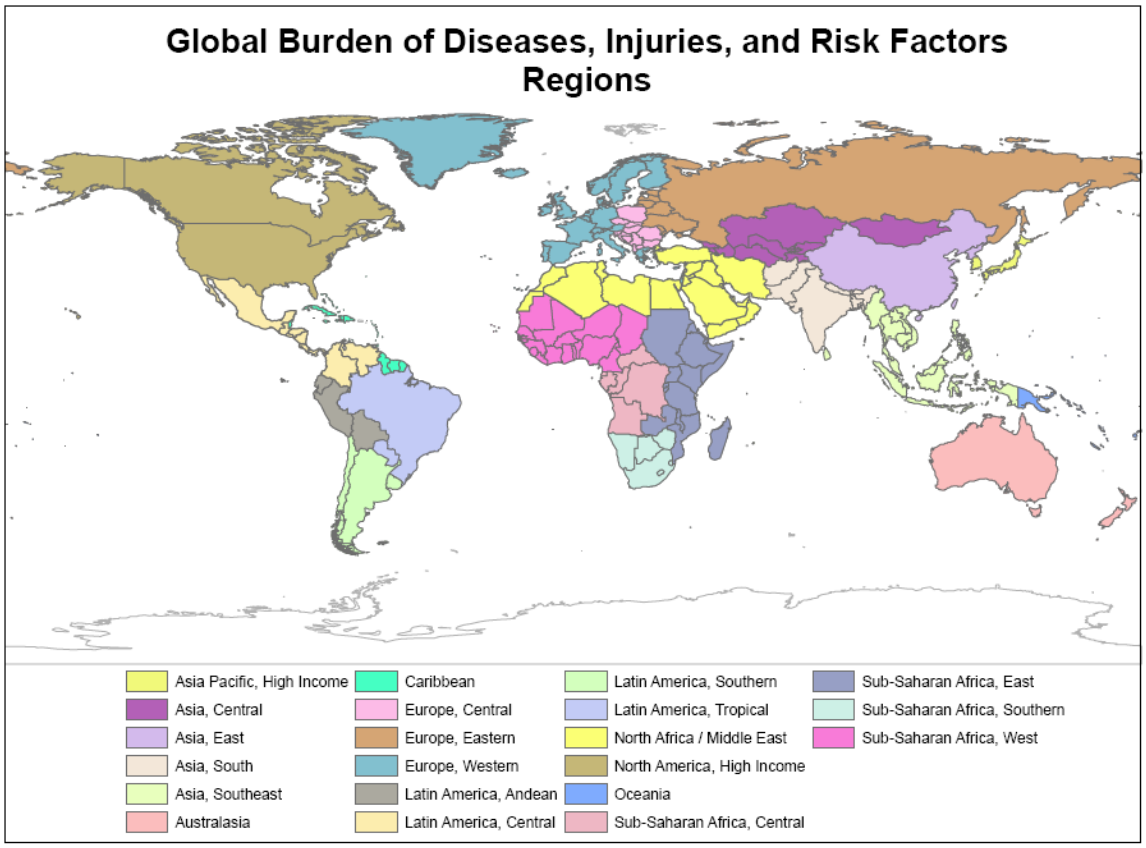

Figure S1. GBD Regions. Reprinted with permission from http://www.globalburden.org/GBD_Study_Operations_Manual_Jan_20_2009.pdf

Population-weighting

Population weighting and assignment of population values to each grid cell was conducted by the following procedure:

1) Input gridded population of the world (GPWv3) values for 1990 and 2005. These are at a resolution of 0.0417°, which is finer than the air pollution (AVG) estimates which are at 0.1°. That makes each air pollution cell equivalent to 2.4 x 2.4 GPWv3 cells.

2) Aggregate the GPW estimates up to 0.1 degree, including spatial smoothing. For each 0.1°x 0.1° grid cell, the population data were summed five different times, once using the central three cells and once offset by one cell in each (N,S,E,W)direction. The average of the resulting five values was used as the aggregated population estimate for each cell (POP).

3) Multiply POP x AVG for each cell

4) Sum POP and POP x AVG for each region and divide the POPxAVG by POP.

Combining data sources and uncertainty characterization ($PM_{2.5}$)

To fuse TM5 and SAT estimates with available measurements and to derive an approach to estimate uncertainty combined the TM5 and satellite (SAT) estimates for 2005 with the measurement database. A global (as opposed to regional) fusion approach was taken given the need to develop global estimates, including many regions without any measurements. Figure S2 shows (top 2 panels) SAT and TM5 plotted against surface monitoring (both direct measurements of $PM_{2.5}$ and $PM_{2.5}$ values estimated from PM_{10} measurements). We did not account for differences in the measurement protocols across the different regions (such as equilibrating filters at 35% RH in the US, 40% RH in Canada, and 50% RH in the EU). Since the variance increases with the mean, we then log transform the measurements and estimates (bottom 2 panels) and plot these.

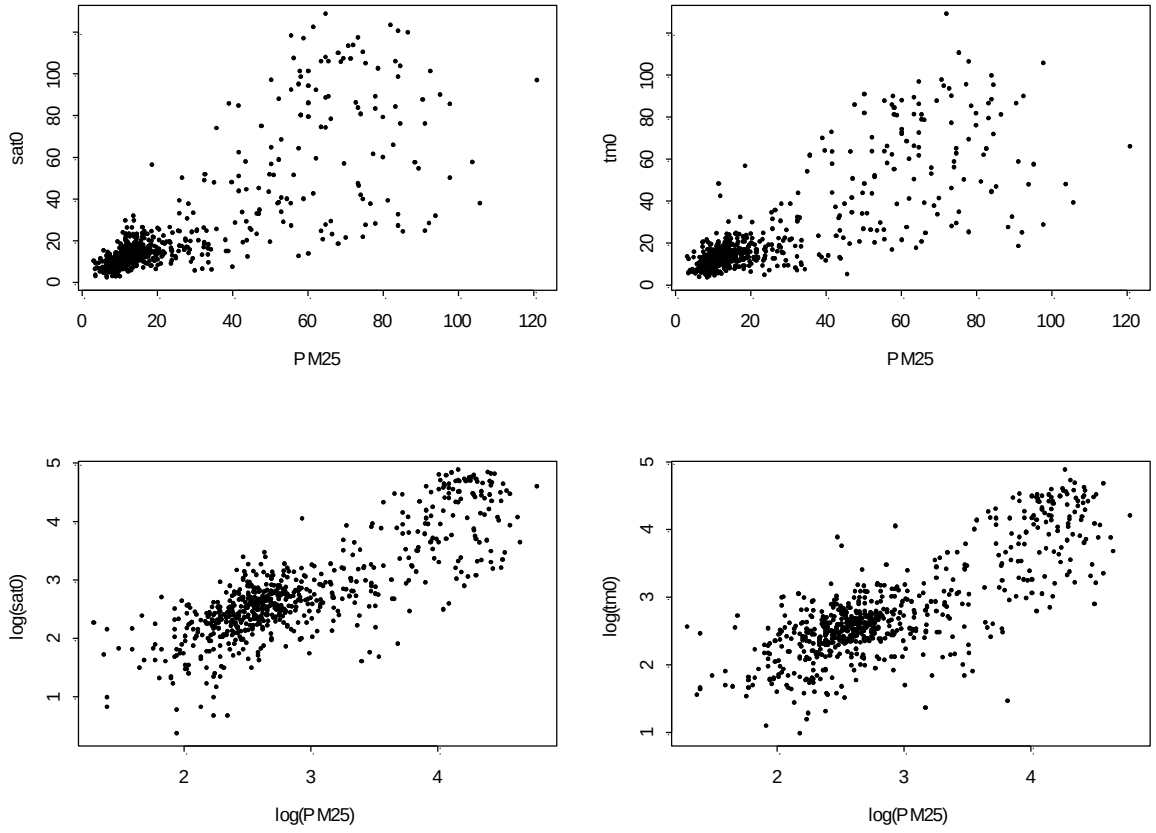

Figure S2. TM5 and SAT estimates with corresponding surface monitoring values of $PM_{2.5}$ (PM25). Note that "PM25" indicates both direct measurements of $PM_{2.5}$ and $PM_{2.5}$ values estimated from PM_{10} measurements, as described in the text and Supporting Information.

As it is apparent that there is deviation from linearity at low concentrations, we sub-divided the data for values < 10 µg/m^3

We next fit the following models (restricted to measured values >10 µg/m^3

$\log(PM_{2.5}) = a + b*\log(\text{SAT or TM5})$;

$\log(PM_{2.5}) = a + b*\log(\text{SAT}) + c*\log(\text{TM5})$

$$\log(PM_{2.5}) = a + b*AVG(SAT,TM5)$$

All three models fits were very similar close with slight improvement in the model using the average of SAT and TM5. This indicates no clear advantage of either TM5 or SAT in comparison with the available ground monitoring values. The R^2 is 0.71 (compared to R^2=0.55 if monitoring values < 10 µg/m^3 are included).

Figure S3 shows the prediction model

$$PM_{2.5} = 1.32*AVG^{0.922}$$

where AVG=average of SAT and TM5 values (on the $PM_{2.5}$ scale). The deviation from the 1:1 line (dashed) indicates a nearly linear prediction of AVG compared to measurements.

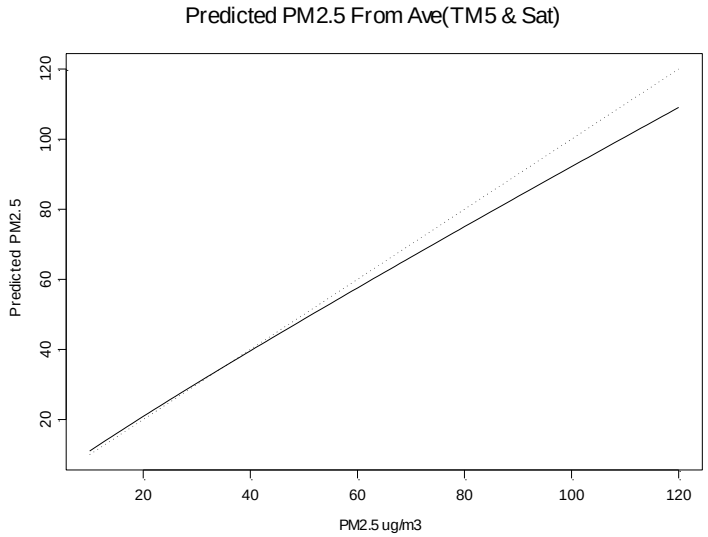

Figure S3. Comparison of ground monitoring and predicted (from TM5 and SAT) annual (2005) average $PM_{2.5}$ concentrations. The prediction is shown by the dotted line compared to a 1:1 (solid) line.

Both estimation approaches (SAT and TM5) therefore closely agree with the monitoring values when > 10 µg/m^3. Given the counterfactual value of 4 µg/m^3, in the actual estimates of disease burden a random value between 4 and 10 is generated for those grid cells with estimates (AVG) between 4 and 10 µg/m^3

From the above prediction model, the prediction error was calculated. The error is nearly all due to residual error since the large sample size leads to very small model error. The ratio of prediction error/predicted value ranged from 8.3% to 15.9% over the log (average) values, which is a relatively small error compared to other components of the burden estimation (risk function). This error is small relative to other sources of error in the overall burden estimates.

While formal uncertainty analysis in the GBD estimates incorporates additional uncertainty (for example, in the concentration-response functions) an approach to characterize exposure

uncertainty would be to generate multiple replicated random values representing mean and uncertainty in exposure estimates for each grid cell in the following manner:

1. When AVG<10 $\mu g/m^3$ generate a random number from a Uniform distribution with bounds 0 and 10 $\mu g/m^3$,
2. When AVG≥10 $\mu g/m^3$, generate a random number from a normal distribution with mean log(AVE) and variance 0.1483 (the residual error of the prediction model) and then take the exponential of this randomly generated number.
3. Calibrate the TM5/SAT data to ground based monitoring data by generating a random number from a normal distribution with mean log(1.32) + 0.922*log(AVG) and variance 0.1483 and then take the exponential of this randomly generated number, only when AVG≥10 $\mu g/m^3$.

Figures S4 and S5 show the global distribution of the individual grid-cell absolute and proportional differences in the 2005 SAT and TM5 estimates of $PM_{2.5}$. As expected there is some trend for greater absolute differences in areas of higher pollution, although this is not universal.

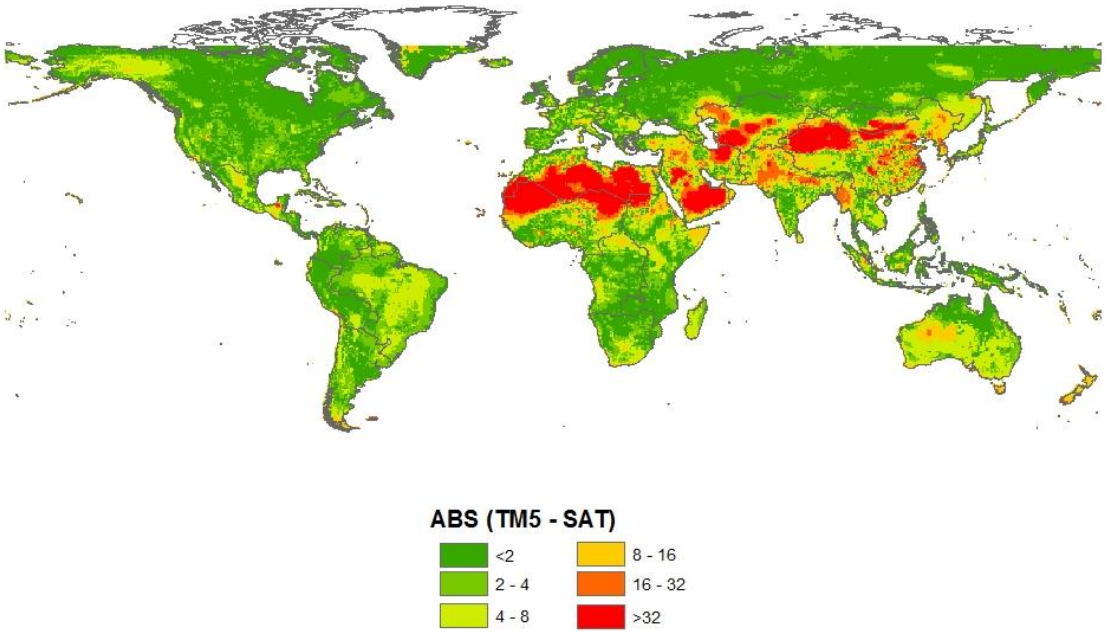

Figure S4. Global distribution of absolute differences ($\mu g/m^3$) between TM5 and SAT estimates of $PM_{2.5}$ for 2005.

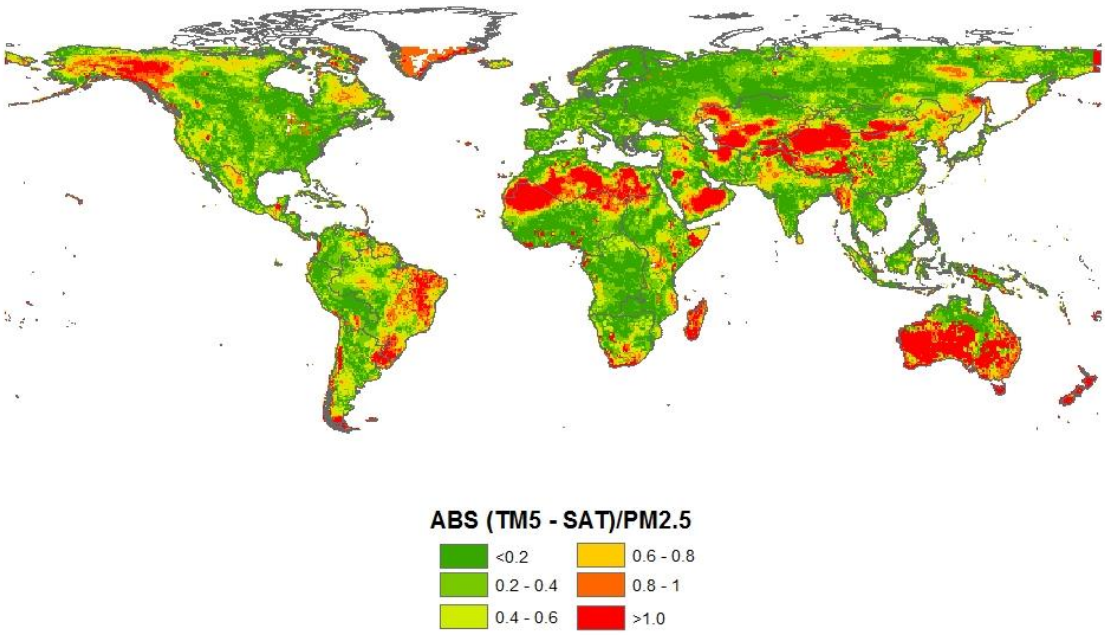

Figure S5. Global distribution of proportional (absolute value of difference between TM5 and SAT divided by final estimates [the average of TM5 and SAT calibrated with the prediction model]) differences in SAT and TM5 estimates of $PM_{2.5}$ for 2005.

While this approach provides an indirect estimate of uncertainty, there is also inherent uncertainty and potential bias in the approaches themselves. Uncertainty in satellite-derived $PM_{2.5}$ results from inaccuracy in both the model and satellite AOD measurements. As part of the aforementioned filtering process, mean satellite AOD error has been limited to 0.1 or 25%. Accuracy of the $PM_{2.5}$/AOD ratio is dominated by the relative vertical structure of the model (7). Based on a comparison with extinction profiles from the CALIPSO satellite, it is estimated that the simulated fraction of AOD within the boundary layer is accurate within 15% (32). The overall error for annual mean coincident satellite-derived $PM_{2.5}$ is estimated to be ± 25%.

Incomplete daily global satellite sampling, caused by cloud-cover and/or instrument limitations, has the potential to introduce sampling bias into annual mean satellite-derived $PM_{2.5}$. Comparisons of continuously and coincidently-sampled simulated $PM_{2.5}$ estimate that satellite-derived $PM_{2.5}$ sampling is sufficient to represent true annual $PM_{2.5}$ to within ± 20%. In a few cases, however, this bias can increase to as much as ± 50%, where major seasonal cycles preside (e.g. South American and Central African biomass burning). In all cases, however, a correction has been applied to account for these differences which should further minimize their impact.

All of these factors can be combined into a total uncertainty estimate as described previously (10)) . The overall PM2.5 uncertainty is estimated to be ±25% which results in a mean global, population-weighted uncertainty of 6.7 $\mu g/m^3$ $PM_{2.5}$. Uncertainty in the satellite-based estimates is highest in regions with substantial landscape fires (Amazon basin, Central Africa, SE Asia) as well as high latitude regions of Asia and North America.

For TM5, multi-factor sensitivity analysis or error-propagation of all processes has not been performed because of the high computational cost. The performance of the model is evaluated by evaluating the different modules (emission, vertical and horizontal transport, chemical and physical processes, wet and dry deposition) with measured data and through multi-model intercomparison exercises. For example, TM5 has participated in "AEROCOM", an international ongoing initiative since 2003 where the performance of global and regional aerosol (PM) models and their key input parameters are evaluated with a focus on climate impacts (33, 34).

In addition, we used the HTAP model comparison to provide summaries of model estimates and standard deviations for TM5 compared to other global chemical transport models included in HTAP (GEOSChem, MOZART, LLNL [Lawrence Livermore National Laboratory] and EMEP [run only for the Northern Hemisphere, so no global estimates]) for major PM components (the HTAP model comparison did not provide PM mass) for 4 populated regions (Figure S6) as examples. The aim of this exercise was to provide some information on how much the TM5 model estimates would have differed using a completely different set of parameterizations.

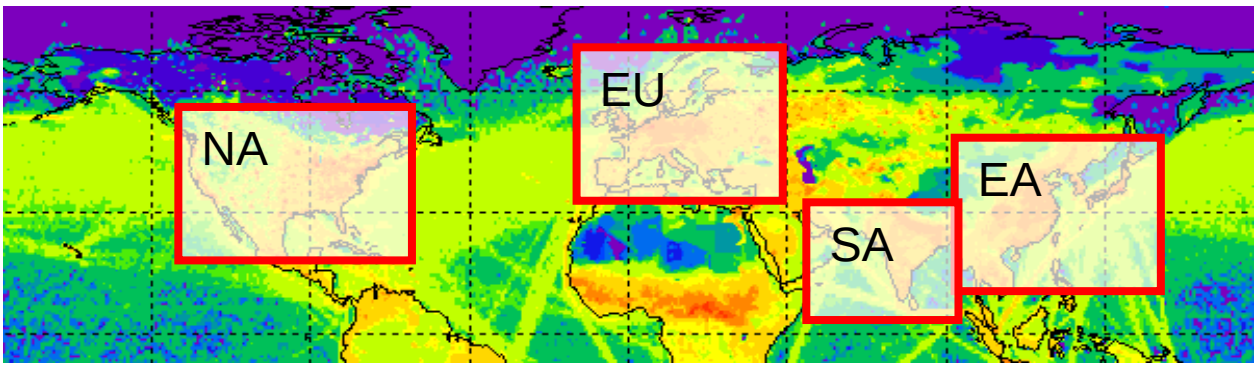

Figure S6. Example regions used for HTAP model comparison (Table S3).

On a global basis, for all constituents except particulate organic matter, TM5 estimates were within the range of estimates provided by other models. For particulate organic matter, estimates from all of the models varied substantially (relative standard deviation of 0.41) with TM5 providing the highest estimates. Globally, relative standard deviations were largest for particulate organic matter and Black Carbon and substantially lower for ozone and sulphate. There were no regions with consistently larger relative standard deviations.

For TM5 (as with other global chemical transport models) the following parameters/processes are believed to be the most influential in the resulting PM concentration estimates: i) emission strength of primary PM (black carbon, primary organic carbon, dust, sea salt); ii) emission of

gaseous precursors for secondary PM (SO_2, NOx, VOC, NH_3); iii) removal rate of PM (wet deposition); iv) horizontal resolution of the model; v)physical-chemical processes leading to the formation of secondary PM from gaseous precursors (in particular secondary organic matter); vi)sub-grid urban increment parameterization; and vii) the PM size distribution and derived $PM_{2.5}$ fraction. For ozone, model estimates are sensitive to assumptions regarding: i) VOC emissions (moreso than NOx emissions); ii) photolysis rates; iii) the vertical gradient within the surface layer; iv) horizontal gradients within a grid box (titration effect by NOx in urban areas, effect of heterogeneous land surface); and v)dry deposition (deposition to vegetation).

Model	Global				NA				EU				SA				EA			
	BC	SO4	POM	O3	BC	SO4	POM	O3	BC	SO4	POM	O3	BC	SO4	POM	O3	BC	SO4	POM	O3
TM5	0.10	0.66	0.77	30.6	0.16	1.26	1.11	42.3	0.28	2.42	0.85	44.3	0.43	2.54	2.24	42.6	0.45	2.03	1.50	38.0
GEOSChem	0.07	0.71	0.40	28.1	0.15	1.35	0.57	40.1	0.18	3.06	0.40	41.9	0.21	1.52	0.86	43.0	0.33	2.13	0.90	39.6
MOZART	0.12	0.72	0.59	27.4	0.22	1.70	1.14	38.6	0.73	2.95	2.81	38.5	0.46	1.30	1.87	42.4	0.61	2.74	2.94	38.7
LLNL	0.05	0.54	0.29	31.0	0.07	1.06	0.43	40.3	0.14	2.44	0.46	42.5	0.23	2.02	1.25	47.9	0.24	1.71	0.71	38.7
EMEP	NA	NA	NA	NA	NA	1.11	NA	40.6	NA	2.52	NA	41.6	NA	2.25	NA	42.2	NA	2.54	NA	38.9
Mean	0.09	0.66	0.51	29.3	0.15	1.30	0.81	40.4	0.33	2.68	1.13	41.8	0.33	1.93	1.55	43.6	0.41	2.23	1.51	38.8
SD	0.03	0.08	0.21	1.8	0.06	0.26	0.37	1.3	0.27	0.30	1.14	2.1	0.13	0.51	0.62	2.4	0.16	0.41	1.01	0.5
RSD	0.37	0.13	0.41	0.06	0.41	0.20	0.45	0.03	0.82	0.11	1.01	0.05	0.39	0.26	0.40	0.06	0.39	0.19	0.67	0.01

Table S3. HTAP model comparison did not provide PM mass) for major PM components (HTAP comparison did not provide PM mass) in 4 populated regions (Figure S4). Comparison of TM5 with GEOSChem, MOZART, LLNL [Lawrence Livermore National Laboratory] and EMEP [run only for the Northern Hemisphere, so no global estimates]) model estimates of annual average Black Carbon (BC, ug/kg air), Sulfate (SO4, ug/kg air), particulate organic matter (POM, ug/kg air), and annual average daily maximum ozone (O3, ppb). Global estimates are provided along with separate estimates and summary statistics (mean, standard deviation, and relative standard deviation) for the 4 regions in the above figure. NA indicates estimates not generated for this model or region.

Counterfactual values

By definition, counterfactual values are choices and there is no right value, but we considered a number of possible approaches including i) Estimation of a "natural background". This could be the lowest (globally applicable) measured concentration, for example, based on the approach(es) used to estimate exposure (the lowest grid cell concentration estimates) or the lowest concentration in the measurement database (including those at "background" measurement sites), ii) the lowest achievable concentration in populated areas (e.g. the lowest measured concentration for an urban area as determined by measurements or the fused estimates), such as the lowest concentration in any grid cell that includes population density above a pre-determined (low population density) threshold, iii) the model estimated concentration in the absence of anthropogenic sources, as described above, iv) historical background levels (as in (35)), calculated with an emissions-based chemical transport model v) the level above which health impacts can be measured with confidence (as in (28)). Such a level could be determined empirically from the studies that are used to develop the concentration-response function for air pollution, or could be based upon the WHO Air Quality Guidelines (36), health-based guidelines, that are designed to be globally applicable.

Ultimately we decided to base the counterfactual on the lowest reported annual average concentration in "populated areas" as a feasible level (approach ii above). For $PM_{2.5}$ this is 4 $\mu g/m^3$, corresponding to measured (2005) annual average concentrations in, Wellington New Zealand (4.1 $\mu g/m^3$, population 370,000), Toowoomba Australia (4.1 $\mu g/m^3$ population 95,000), Santa Fe USA (4.5 $\mu g/m^3$ population 147,000), Cheyenne USA (4.1 $\mu g/m^3$ population 81,000). This decision was also based on the methodology used in the GBD estimates by which multiple

counterfactual values (i.e. WHO Air Quality Guidelines, lowest level at which effects have been observed in epidemiologic studies) will be evaluated in sensitivity analyses and by a procedure to harmonize the basis for counterfactual value selection across different risk factors (i.e. the approach applied to select a counterfactual for high blood pressure, cholesterol and outdoor air pollution should be similar).

For outdoor air pollution, selection of counterfactual values are further complicated by regional variation and specifically for PM, the influence of windblown dust is important. We elected to use a single global counterfactual value as there are several analyses indicating increased desertification (in the Sahara) over time related to anthropogenic activity (37, 38). This suggests that, in theory, reduced desertification and therefore reduced windblown dust is achievable. Further, there are examples in the western U.S. (and more recently in China and Thailand) where air quality management measures have been implemented with some success to specifically reduce windblown dust levels, suggesting that lower levels of airborne dust are achievable.

Estimation of a counterfactual for ozone is complicated by the natural sources of ozone and its precursors, and the variation in baseline levels. To be consistent with the approach applied to $PM_{2.5}$, selection of the ozone counterfactual was based on a level that is measured in a very low-ozone city. In the case of the nationwide ozone database used for the Jerrett et al. study (39), the lowest annual ozone level was found in Honolulu, HI, (population 876,000) which had a metropolitan area annual average of 22 ppb (43 $\mu g/m^3$) during the period considered in this study. This compares well with the annual average ozone levels recorded at remote areas around the world, such as Pt. Barrow, AK (23-29 ppb, 45 – 57 $\mu g/m^3$) (40), although even lower levels

may be present elsewhere. As with $PM_{2.5}$, any burden estimates for ozone will include sensitivity analyses evaluating other counterfactual levels.

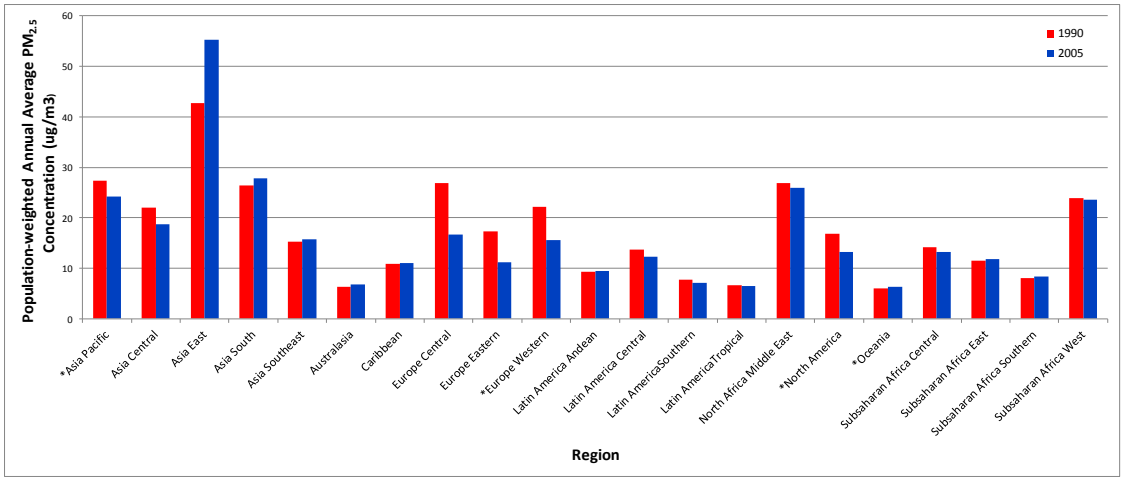

Figure S7. Comparison of 1990 and 2005 annual average population–weighted regional $PM_{2.5}$ exposure estimates ($\mu g/m^3$). *High income region.

References

1. Dentener, F.; Stevenson, D.; Ellingsen, K.; van Noije, T.; Schultz, M.; Amann, M.; Atherton, C.; Bell, N.; Bergmann, D.; Bey, I.; Bouwman, L.; Butler, T.; Cofala, J.; Collins, B.; Drevet, J.; Doherty, R.; Eickhout, B.; Eskes, H.; Fiore, A.; Gauss, M.; Hauglustaine, D.; Horowitz, L.; Isaksen, I.S.A.; Josse, B.; Lawrence, M.; Krol, M.; Lamarque, J.F.; Montanaro, V.; Muller, J.F.; Peuch, V.H.; Pitari, G.; Pyle, J.; Rast, S.; Rodriguez, J.; Sanderson, M.; Savage, N.H.; Shindell, D.; Strahan, S.; Szopa, S.; Sudo, K.; Van Dingenen, R.; Wild, O.; Zeng, G. The global atmospheric environment for the next generation. *Environ. Sci. Technol.* **2006,** *40,* 3586-3594.

2. Krol, M.; Houweling, S.; Bregman, B.; van den Broek, M.; Segers, A.; van Velthoven, P.; Peters, W.; Dentener, F.; Bergamaschi, P. The two-way nested global chemistry-transport zoom model TM5: algorithm and applications. *Atmospheric Chemistry and Physics* **2005,** *5,* 417-432.

3. Van Aardenne, J.; Dentener, F.; Van Dingenen, R.; Maenhout, G.; Marmer, E.; Vignati, E.; Russ, P.; Szabo, L.; Raes, F. Climate and air quality impacts of combined climate change and air pollution policy applications. **2010,** *EUR 24572 EN - 2010,* 4-4-71.

4. Fiore, A.M.; Dentener, F.J.; Wild, O.; Cuvelier, C.; Schultz, M.G.; Hess, P.; Textor, C.; Schulz, M.; Doherty, R.M.; Horowitz, L.W.; MacKenzie, I.A.; Sanderson, M.G.; Shindell, D.T.; Stevenson, D.S.; Szopa, S.; Van Dingenen, R.; Zeng, G.; Atherton, C.; Bergmann, D.; Bey, I.; Carmichael, G.; Collins, W.J.; Duncan, B.N.; Faluvegi, G.; Folberth, G.; Gauss, M.; Gong, S.; Hauglustaine, D.; Holloway, T.; Isaksen, I.S.A.; Jacob, D.J.; Jonson, J.E.; Kaminski, J.W.; Keating, T.J.; Lupu, A.; Marmer, E.; Montanaro, V.; Park, R.J.; Pitari, G.; Pringle, K.J.; Pyle, J.A.; Schroeder, S.; Vivanco, M.G.; Wind, P.; Wojcik, G.; Wu, S.; Zuber, A. Multimodel estimates of intercontinental source-receptor relationships for ozone pollution. *Journal of Geophysical Research-Atmospheres* **2009,** *114,* 1-21.

5. Lamarque, J.F.; Bond, T.C.; Eyring, V.; Granier, C.; Heil, A.; Klimont, Z.; Lee, D.; Liousse, C.; Mieville, A.; Owen, B.; Schultz, M.G.; Shindell, D.; Smith, S.J.; Stehfest, E.; Van Aardenne, J.; Cooper, O.R.; Kainuma, M.; Mahowald, N.; McConnell, J.R.; Naik, V.; Riahi, K.; van Vuuren, D.P. Historical (1850-2000) gridded anthropogenic and biomass burning emissions of reactive gases and aerosols: methodology and application. *Atmospheric Chemistry and Physics* **2010,** *10,* 7017-7039.

6. Liu, Y.; Park, R.J.; Jacob, D.J.; Li, Q.B.; Kilaru, V.; Sarnat, J.A. Mapping annual mean ground-level PM2.5 concentrations using Multiangle Imaging Spectroradiometer aerosol optical thickness over the contiguous United States. *Journal of Geophysical Research-Atmospheres* **2004,** *109,* D22206-1-10.

7. van Donkelaar, A.; Martin, R.V.; Park, R.J. Estimating ground-level PM2.5 using aerosol optical depth determined from satellite remote sensing. *Journal of Geophysical Research-Atmospheres* **2006,** *111,*

8. Holben, B.N.; Eck, T.F.; Slutsker, I.; Tanre, D.; Buis, J.P.; Setzer, A.; Vermote, E.; Reagan, J.A.; Kaufman, Y.J.; Nakajima, T.; Lavenu, F.; Jankowiak, I.; Smirnov, A. AERONET - A federated instrument network and data archive for aerosol characterization. *Remote Sens. Environ.* **1998,** *66,* 1-16.

9. Lucht, W.; Schaaf, C.B.; Strahler, A.H. An algorithm for the retrieval of albedo from space using semiempirical BRDF models. *IEEE Trans. Geosci. Remote Sens.* **2000,** *38,* 977-998.

10. van Donkelaar, A.; Martin, R.V.; Brauer, M.; Kahn, R.; Levy, R.; Verduzco, C.; Villeneuve, P.J. Global estimates of ambient fine particulate matter concentrations from satellite-based aerosol optical depth: development and application. *Environ. Health Perspect.* **2010,** *118,* 847-855.

11. Park, R.J.; Jacob, D.J.; Kumar, N.; Yantosca, R.M. Regional visibility statistics in the United States: Natural and transboundary pollution influences, and implications for the Regional Haze Rule. *Atmos. Environ.* **2006,** *40,* 5405-5423.

12. Park, R.J.; Jacob, D.J.; Chin, M.; Martin, R.V. Sources of carbonaceous aerosols over the United States and implications for natural visibility. *Journal of Geophysical Research-Atmospheres* **2003,** *108,* D12, 4355,-5-1 - 5-12.

13. Liao, H.; Henze, D.K.; Seinfeld, J.H.; Wu, S.L.; Mickley, L.J. Biogenic secondary organic aerosol over the United States: Comparison of climatological simulations with observations. *Journal of Geophysical Research-Atmospheres* **2007,** *112,* D06201-1-19.

14. Fairlie, T.D.; Jacob, D.J.; Park, R.J. The impact of transpacific transport of mineral dust in the United States. *Atmos. Environ.* **2007,** *41,* 1251-1266.

15. Alexander, B.; Park, R.J.; Jacob, D.J.; Li, Q.B.; Yantosca, R.M.; Savarino, J.; Lee, C.C.W.; Thiemens, M.H. Sulfate formation in sea-salt aerosols: Constraints from oxygen isotopes. *Journal of Geophysical Research-Atmospheres* **2005,** *110,* 1-12.

16. Pye, H.O.T.; Liao, H.; Wu, S.; Mickley, L.J.; Jacob, D.J.; Henze, D.K.; Seinfeld, J.H. Effect of changes in climate and emissions on future sulfate-nitrate-ammonium aerosol levels in the United States. *Journal of Geophysical Research-Atmospheres* **2009,** *114,* D01205-1-18.

17. Heald, C.L.; Jacob, D.J.; Park, R.J.; Alexander, B.; Fairlie, T.D.; Yantosca, R.M.; Chu, D.A. Transpacific transport of Asian anthropogenic aerosols and its impact on surface air quality in the United States. *Journal of Geophysical Research-Atmospheres* **2006,** *111,*

18. Drury, E.; Jacob, D.J.; Spurr, R.J.D.; Wang, J.; Shinozuka, Y.; Anderson, B.E.; Clarke, A.D.; Dibb, J.; McNaughton, C.; Weber, R. Synthesis of satellite (MODIS), aircraft (ICARTT), and surface (IMPROVE, EPA-AQS, AERONET) aerosol observations over eastern North America to improve MODIS aerosol retrievals and constrain surface aerosol concentrations and sources. *Journal of Geophysical Research-Atmospheres* **2010,** *115,* D14204-1-17.

19. Heald, C.L.; Jacob, D.J.; Park, R.J.; Russell, L.M.; Huebert, B.J.; Seinfeld, J.H.; Liao, H.; Weber, R.J. A large organic aerosol source in the free troposphere missing from current models. *Geophys. Res. Lett.* **2005,** *32,* L18809-1-4.

20. van Donkelaar, A.; Martin, R.V.; Leaitch, W.R.; Macdonald, A.M.; Walker, T.W.; Streets, D.G.; Zhang, Q.; Dunlea, E.J.; Jimenez, J.L.; Dibb, J.E.; Huey, L.G.; Weber, R.; Andreae, M.O. Analysis of aircraft and satellite measurements from the Intercontinental Chemical Transport Experiment (INTEX-B) to quantify long-range transport of East Asian sulfur to Canada. *Atmospheric Chemistry and Physics* **2008,** *8,* 2999-3014.

21. Dunlea, E.J.; DeCarlo, P.F.; Aiken, A.C.; Kimmel, J.R.; Peltier, R.E.; Weber, R.J.; Tomlinson, J.; Collins, D.R.; Shinozuka, Y.; McNaughton, C.S.; Howell, S.G.; Clarke, A.D.; Emmons, L.K.; Apel, E.C.; Pfister, G.G.; van Donkelaar, A.; Martin, R.V.; Millet, D.B.; Heald, C.L.; Jimenez, J.L. Evolution of Asian aerosols during transpacific transport in INTEX-B. *Atmospheric Chemistry and Physics* **2009,** *9,* 7257-7287.

22. Olivier, J.G.J.; Peters, J.A.H.W.; Bakker, J.; Berdowski, J.J.M.; Visschedijk, A.J.H.; Bloos, J.J. EDGAR 3.2: Reference database with trend data of global greenhouse gas emissions for 1970-1995. *Non-C02 Greenhouse Gases: Scientific Understanding, Control Options and Policy Aspects* **2002,** 291-292.

23. Kuhns, H.; Knipping, E.M.; Vukovich, J.M. Development of a United States-Mexico emissions inventory for the Big Bend Regional Aerosol and Visibility Observational (BRAVO) Study. *J. Air Waste Manage. Assoc.* **2005,** *55,* 677-692.

24. Streets, D.G.; Bond, T.C.; Carmichael, G.R.; Fernandes, S.D.; Fu, Q.; He, D.; Klimont, Z.; Nelson, S.M.; Tsai, N.Y.; Wang, M.Q.; Woo, J.H.; Yarber, K.F. An inventory of gaseous and primary aerosol emissions in Asia in the year 2000. *Journal of Geophysical Research-Atmospheres* **2003,** *108,*

25. Streets, D.G.; Zhang, Q.; Wang, L.T.; He, K.B.; Hao, J.M.; Wu, Y.; Tang, Y.H.; Carmichael, G.R. Revisiting China's CO emissions after the Transport and Chemical Evolution over the Pacific (TRACE-P) mission: Synthesis of inventories, atmospheric modeling, and observations. *Journal of Geophysical Research-Atmospheres* **2006,** *111,*

26. Benkovitz, C.M.; Scholtz, M.T.; Pacyna, J.; Tarrason, L.; Dignon, J.; Voldner, E.C.; Spiro, P.A.; Logan, J.A.; Graedel, T.E. Global gridded inventories of anthropogenic emissions of sulfur and nitrogen. *Journal of Geophysical Research-Atmospheres* **1996,** *101,* 29239-29253.

27. Bond, T.C.; Streets, D.G.; Yarber, K.F.; Nelson, S.M.; Woo, J.H.; Klimont, Z. A technology-based global inventory of black and organic carbon emissions from combustion. *Journal of Geophysical Research-Atmospheres* **2004,** *109,*

28. Cohen AJ; Anderson HR; Ostro B; Pandey KD; Krzyzanowski M; Kuenzli N; Gutschmidt K; Pope, C.I.; Romieu, I.; Samet J.M.; Smith, K.R. Urban Air Pollution, In *Comparative Quantification of Health Risks: Global and Regional Burden of Disease Attributable to Selected*

Major Risk Factors, 1st ed.; Ezzati M, Rodgers AD, Lopez AD and Murray CJL, Eds.; World Health Organization: Geneva, 2004; Vol.2 pp. 1353-1453.

29. Brown, K.W.; Bouhamra, W.; Lamoureux, D.P.; Evans, J.S.; Koutrakis, P. Characterization of particulate matter for three sites in Kuwait. *J. Air Waste Manage. Assoc.* **2008,** *58*, 994-1003.

30. Kouyoumdjian, H. and Saliba, N.A. Mass concentration and ion composition of coarse and fine particles in an urban area in Beirut: effect of calcium carbonate on the absorption of nitric and sulfuric acids and the depletion of chloride. *Atmospheric Chemistry and Physics* **2006,** *6*, 1865-1877.

31. Hopke, P.K.; Cohen, D.D.; Begum, B.A.; Biswas, S.K.; Ni, B.F.; Pandit, G.G.; Santoso, M.; Chung, Y.S.; Davy, P.; Markwitz, A.; Waheed, S.; Siddique, N.; Santos, F.L.; Pabroa, P.C.B.; Seneviratne, M.C.S.; Wimolwattanapun, W.; Bunprapob, S.; Vuong, T.B.; Hien, P.D.; Markowicz, A. Urban air quality in the Asian region. *Sci. Total Environ.* **2008,** *404*, 103-112.

32. Vaughan, M.; Young, S.; Winker, D.; Powell, K.; Omar, A.; Liu, Z.Y.; Hu, Y.X.; Hostetler, C. Fully automated analysis of space-based lidar data: an overview of the CALIPSO retrieval algorithms and data products. *Laser Radar Techniques for Atmospheric Sensing* **2004,** *5575*, 16-30.

33. Schulz, M.; Textor, C.; Kinne, S.; Balkanski, Y.; Bauer, S.; Berntsen, T.; Berglen, T.; Boucher, O.; Dentener, F.; Guibert, S.; Isaksen, I.S.A.; Iversen, T.; Koch, D.; Kirkevag, A.; Liu, X.; Montanaro, V.; Myhre, G.; Penner, J.E.; Pitari, G.; Reddy, S.; Seland, O.; Stier, P.; Takemura, T. Radiative forcing by aerosols as derived from the AeroCom present-day and pre-industrial simulations. *Atmospheric Chemistry and Physics* **2006,** *6*, 5225-5246.

34. Textor, C.; Schulz, M.; Guibert, S.; Kinne, S.; Balkanski, Y.; Bauer, S.; Berntsen, T.; Berglen, T.; Boucher, O.; Chin, M.; Dentener, F.; Diehl, T.; Easter, R.; Feichter, H.; Fillmore, D.; Ghan, S.; Ginoux, P.; Gong, S.; Kristjansson, J.E.; Krol, M.; Lauer, A.; Lamarque, J.F.; Liu, X.; Montanaro, V.; Myhre, G.; Penner, J.; Pitari, G.; Reddy, S.; Seland, O.; Stier, P.; Takemura, T.; Tie, X. Analysis and quantification of the diversities of aerosol life cycles within AeroCom. *Atmospheric Chemistry and Physics* **2006,** *6*, 1777-1813.

35. Anenberg, S.C.; Horowitz, L.W.; Tong, D.Q.; West, J.J. An Estimate of the Global Burden of Anthropogenic Ozone and Fine Particulate Matter on Premature Human Mortality Using Atmospheric Modeling. *Environ. Health Perspect.* **2010,** *118*, 1189-1195.

36. World Health Organization ***Air quality guidelines. Global update 2005. Particulate Matter, Ozone, Nitrogen Dioxide and Sulfur Dioxide***. World Health Organization: 2006;

37. Mulitza, S.; Heslop, D.; Pittauerova, D.; Fischer, H.W.; Meyer, I.; Stuut, J.B.; Zabel, M.; Mollenhauer, G.; Collins, J.A.; Kuhnert, H.; Schulz, M. Increase in African dust flux at the onset of commercial agriculture in the Sahel region. *Nature* **2010,** *466*, 226-228.

38. Okin, G.S.; Bullard, J.E.; Reynolds, R.L.; Ballantine, J.C.; Schepanski, K.; Todd, M.C.; Belnap, J.; Baddock, M.C.; Gill, T.E.; Miller, M.E. Dust: Small-scale processes with global consequences. *Eos Trans. AGU* **2011,** *92,*

39. Jerrett, M.; Burnett, R.T.; Pope, C.A.,3rd; Ito, K.; Thurston, G.; Krewski, D.; Shi, Y.; Calle, E.; Thun, M. Long-term ozone exposure and mortality. *N. Engl. J. Med.* **2009,** *360,* 1085-1095.

40. Vingarzan, R. A review of surface ozone background levels and trends. *Atmos. Environ.* **2004,** *38,* 3431-3442.